NMR MONITORING OF SPONTANEOUS BRINE IMBIBITION IN CARBONATES

Haldis Riskedal[1], Lejla Tipura[1], James Howard[2] and Arne Graue[1]
[1]University of Bergen, Bergen, Norway
[2]ConocoPhillips, Bartlesville, OK, USA

This paper was prepared for presentation at the International Symposium of the Society of Core Analysts held in Abu Dhabi, UAE 29 October-2 November, 2008

ABSTRACT

Laboratory NMR measurements of relaxation times were used to monitor changes in saturation during spontaneous brine imbibition in a set of carbonate core plugs with complex pore geometry. Saturation measurements require separate and distinguishable NMR contributions from the water and oil. One challenge was to separate the NMR relaxation contribution of the water-filled porosity found in a broad range of pore sizes from the hydrocarbon components. One approach to reduce the overlap in relaxation signals was to replace the H_2O with D_2O. This made it possible to measure only the T_2 oil contribution. In earlier work we reported a new method to measure in-situ wettabilities based on relative shifts in T_2 relaxation times. Isolating the NMR contributions from oil and water would also have benefits for this method.

In several spontaneous brine imbibition experiments using H_2O and D_2O, the imbibition process was monitored with T_2 distributions collected for the whole core plug. Attempts to create baseline experiments revealed difficulties in obtaining reproducible fluid saturation development and imbibition endpoints. 3D MRI images of forced water imbibition were obtained and indicated dispersed waterfronts during the flooding. However, these results did not fully explain the observed T_2 distributions and shifts in relaxation times measured at various fluid saturations. We speculate that this was due to porosity heterogeneities in this carbonate rock and thus may provide more pronounced hysteresis effects.

Efforts to measure NMR properties in selected transverse slices of the core were affected by temperature-dependent diffusion that caused unequal shifts in the relaxation of the non-wetting oil and the remaining water signal in the smaller pores. The gradient-controlled slice measurements of relaxation properties therefore were not directly comparable to the relaxation time distributions measured in a uniform field, though many similarities were observed.

INTRODUCTION

Nuclear Magnetic Resonance (NMR) studies have shown that transverse relaxation time (T_2) measurements of sandstone, limestone and chalk samples saturated with water and oil

are strongly dependent on the wettability, Johannesen *et al.*, (2006, 2007) and fluid saturations, Straley *et al*., (1995), Ding *et* al. (2006), Chang and Ioannidis, (2002) of each sample. The interpretation of the relaxation time distributions of limestone samples have proven to be more challenging than with chalk and sandstone because of their more complex pore geometry. Several approaches are available to clarify the T_2 distributions associated with limestone samples so to simplify the interpretation. One method is to displace the water (H_2O) in the pores with deuterium oxide (D_2O), which is not detected by a standard NMR experiment tuned to hydrogen. The displacement of the water with D_2O leaves the oil as the only hydrogen-bearing fluid in the pores that contributes to the NMR signal.

The measured relaxation time for fluids located in pores is defined as:

$$\frac{1}{T_2} = \left(1 - \frac{\delta \cdot S}{V}\right)\frac{1}{T_{2b}} + \frac{\delta \cdot S}{V}\frac{1}{T_{2s}} + \frac{\left(\gamma \cdot G \cdot t_E\right)^2 D}{12}, \tag{1}$$

where δ is the thickness of the surface area, S is the surface area, V is the pore volume, T_{2b} is the transverse relaxation time for bulk fluid, T_{2s} is the transverse relaxation time for the surface-enhanced relaxation, γ is the gyromagnetic ratio, G is the magnetic field gradient (assumed to be constant), t_E is the time between echoes and D is the self diffusion coefficient of the fluid. Since the relaxation time for bulk water or light oil is very slow, the first term tends to be very small. The surface-enhance relaxation term is the basis of the interpretation of pore size distributions from NMR measurements where fluid in a pore relaxes at a rate determined by its size and the surface relaxivity, Dunn *et al.*, (2002). Rocks with an assemblage of pore sizes and/or are saturated with more than one type of fluid containing hydrogen therefore have a range of relaxation times that can be extracted from the measured data. The solution of this problem is accomplished with a non-linear least-squares fit to the data with a regularization term that adjusts the fit to the available signal-to-noise levels of the data, Kenyon, (1992), Dunn *et al.*, (2002). The advantage of this approach is a robust solution of relaxation times with a common basis function of relaxation times that allows for easy comparison amongst samples as saturation or wettability are altered.

The third term in Equation (1) defines the contribution of diffusion processes to the measured relaxation time. Since most laboratory measurements are made in a uniform field with no gradients, this diffusion term is often ignored on the assumption that internal gradients in the pores are minimal. Many samples do have some internal gradients that affect the measured relaxation time as the echo spacing, t_E, is altered. In contrast, the use of a constant field gradient while measuring the relaxation time is seldom used in the laboratory though it has significant implications for logging measurements. The application of a constant gradient along one axis of the saturated core sample enhances the diffusion process and provides an opportunity to selectively sample portions of the core. The selection of the resonance frequency of the measurement along with the strength of the

gradient defines the thickness of a transverse slice and its location along the length of the core in which a conventional Carr-Purcell-Meiboom-Gill (CPMG) pulse sequence that is used to measure T_2 relaxation times, Carr and Purcell, (1954), Meiboom and Gill, (1958). These slice-selected CPMG measurements made under gradient conditions are compared with standard CPMG measurements in an effort to describe better the relationships of oil and water relaxation behavior in limestone pore systems with complex geometry and wettability conditions.

PROCEDURES

Fluids

Two types of synthetic formation brine of similar dissolved solid composition were used. The only difference was that H_2O was replaced by D_2O in the second brine. Decane was used as oil phase (Table 1).

Core Plugs

Edwards Limestone core plugs of about 3.8 cm diameter and length of about 6 cm were dried before evacuation and brine saturation. The difference in mass before and after the saturation was the basis for calculation of porosity. Permeability was determined by Darcy's law using the H_2O-based brine with the pressure drop over the core plug being measured at five different flow rates (Table 2). Before the final water saturation was established, the core plugs were drained with decane using approximately 5 pore volumes (PV) flowed in each direction to obtain residual water saturation. The Edwards Limestone is a carbonate from West Texas noted for its broad range of pore types and sizes observed in thin section, including abundant moldic porosity with oversized pores.

T_2 Measurements

NMR measurements were collected during water imbibition in order to investigate changes in T_2 distributions as the water saturation increased. The water-wet core plug, which was drained to residual water saturation, was placed in a beaker of brine. When the imbibition started, the core plug was removed from the beaker and prepared for NMR measurement. These preparations included removing surface droplets with a moisten paper towel and wrapping the core plug in plastic wrap to prevent evaporation. The core plug was then placed in a glass tube in the NMR instrument. The CPMG pulse sequences for no gradient and fixed gradient were used for data collection at each imbibition step. The imbibition was disrupted to obtain T_2 distributions as many times as possible until the imbibition was completed. Every time the core plug was taken out of the imbibition fluid, the weight was recorded in order to calculate the fluid saturations. Amott-Harvey index was calculated based on the residual and spontaneous imbibition end point saturations, Amott, (1959), Boneau and Clampitt, (1977).

MRI Measurements

For one of the core plugs (HR27), D_2O was injected before any decane was introduced to the core. Since the H_2O-D_2O displacement process is miscible, 100% D_2O saturation was assumed. After the D_2O flooding, the core was flooded with decane until it reached

residual water saturation. The sample was placed in a Magnetic Resonance Imaging (MRI) instrument and 3D images were collected with standard spin-echo pulse sequences during the subsequent injection of D_2O at a rate of 0.2 ml/h. The images were collected by repeated cycles constituted by three different scans. As soon as a scan was completed, another one started. Each of the scans lasted for 1.7 hours, meaning that 0.027 PV D_2O was injected between the start of two following scans. Due to different settings in the second scan in each cycle, these images could not be correlated to the rest of the images.

RESULTS AND DISCUSSION

T_2 distributions were obtained during water and oil imbibition for more than 20 Edwards Limestone core plugs with various wettability preferences. The T_2 values for the oil phase at residual water saturation were normalized to values between 0 and 1 where 1 was the slowest measured T_2 value. The normalized T_2 values were plotted versus Amott-Harvey index (Figure 1). The data points form a linear trend, where the T_2 for the oil component decreases as the Amott-Harvey index decreases. The T_2 for the oil phase decreases because larger fraction of the oil phase is in contact with the pore walls as the sample becomes less water-wet, meaning that the contribution from the fast surface relaxation increases, while the contribution from the slow bulk relaxation of the decane decreases. The same observations were done for Portland chalk (squared data points in Figure 1). See Johannesen *et al.*, (2006, 2007) for more details on the wettability dependency of T_2.

It was very difficult to keep track of the material balance during the imbibition process, because the core plugs were frequently removed from the imbibition fluid in order to make the T_2 measurements. Because the Edwards Limestone core plugs have relatively low porosity and there is a relatively small density difference between the brine and decane along with the loss of small pieces of the core plugs during experimental procedures, the result is that mass measurements may not yield very accurate values for fluid saturations. Fluid saturations in chalk calculated based on NMR measurements have shown to give about as good results as those calculated from conventional core analyses, Howard and Spinler, (1995).

But the method of saturation determination by NMR measurements requires separated signal from each of the fluid phases. The fact that Edwards Limestone has more complex pore geometry than chalk is seen by comparing T_2 distributions obtained at 100% water saturated core plugs from the two rocks. There are more peaks in the T_2 distributions of Edwards Limestone, reflecting larger amount of different pore sizes in the porous medium according to Equation (1). Larger amount of different pore sizes increases the possibility of overlapping of signal from the water phase and the oil phase in the core plug, because the relaxation of the water in a specific pore size may be the same as the relaxation of the oil in another pore size, due to different fluid distribution for the various pore sizes.

Two separate water imbibition cycles were performed on two core plugs HR28 and HR29. After the first imbibition cycle in H_2O-based brine was completed, the H_2O in the core plugs was displaced by D_2O. The second imbibition cycle took place in a D_2O-based brine,

in order to isolate the signal from the oil phase at various fluid saturations. T_2 distributions obtained during the first imbibition cycle (H_2O-based brine) in HR29 are shown in Figure 2. The dotted line represents the T_2 distribution for a 40 ml bulk decane sample, with T_2 value of 1381 ± 4 msec. From the T_2 distribution obtained at 100% water saturation, there seems to be three different pore sizes in the core plug. At residual water saturation, the signal intensity from the water phase has decreased and the T_2 for the water phase has shifted towards faster relaxation times. The core plug was not aged and therefore assumed to be strongly water wet, meaning that the water displaced by the introduced oil was mainly located in the centre of the pores. The oil peak at residual water saturation has slightly lower T_2 value than bulk decane, indicating that some of the oil phase is in contact with the pore walls, which is not unlikely if the pores have many sharp edges. At low oil saturations the T_2 for the decane in the core plug becomes larger than bulk decane. This phenomenon is only seen for un-aged Edwards Limestone core plugs at low oil saturations. The explanation may be that there is a type of interaction between the small oil droplets in the centre of the pores and the water phase, reducing the relaxation of the oil phase.

As the H_2O in HR29 is displaced by D_2O at residual oil saturation, the signal from the water phase is suppressed and a shift towards slower relaxation times is observed for the oil phase (Figure 3f). If there is a kind of interaction between the oil and the water at low oil saturations, reducing the relaxation for the oil, this also may be the reason for different T_2 distributions for the two cases with the two different water phases, H_2O and D_2O. By removing the H_2O, the opportunities for the hydrogen in the decane to interact with other hydrogens in the water phase is reduced, giving a reduction in the number of dipole-dipole interactions between hydrogens. This results in slower relaxation rates for those few remaining hydrogens – especially since there are limited interactions with the pore walls when at low oil saturations. The difference in T_2 for the oil phase for H_2O and D_2O as water phase increases as the oil saturation decreases (Figure 3). The agreement of the T_2 values for the oil phase at low water saturations (when the effects from interactions between the water and the oil phase are small) indicates good reproducibility of the T_2 measurements. The same agreement is seen for the core plug HR28. The small, fast peaks in the T_2 distributions obtained with D_2O in HR29 are more likely due to remaining parts of H_2O in the core plug after D_2O flooding, than decane. It is unlikely that the low drainage pressure (1.5 bar/cm core length) allows the oil to intrude the small pores and it is also unlikely that the oil phase in the larger pores are divided in several droplets where some of them have larger contact with the pore walls. NMR scanning of the water production during the H_2O-D_2O displacement indicated about 4% H_2O remaining in HR29. Normally, every signal below 1 ms in the T_2 distribution curves are assumed to be noise, due to increasing noise with decreasing T_2 values. Many of the diagrams in Figure 3 shows small peaks at 2-3 ms, which also may be considered as noise.

The two imbibition cycles for HR28 and HR29 did not result in the same imbibition curves and end point saturations (Figure 4), which is a reflection of the heterogeneity of Edwards Limestone. The comparison of T_2 distribution curves with H_2O and D_2O as water phase therefore had to be performed at same water saturation rather than same imbibition time.

MRI measurements during D_2O flooding of the un-aged Edwards Limestone core plug HR27 also gave indications of a relatively heterogeneous porous medium.

It is seen from Figure 2 that there is a reversed shift in the T_2 for the oil phase after the forced water imbibition. During the spontaneous water imbibition, the T_2 for the oil phase shifts towards higher relaxation times, while the forced imbibition gives a decrease in the T_2 for the oil phase. This observation is obtained for four of ten water imbibition cycles performed on eight different un-aged Edwards Limestone core plugs. These results suggest that the fluid distribution in the pores is altered as different forces act on the fluids. The spontaneous water imbibition is driven by capillary forces, meaning that the oil in the smallest pores will be displaced first. The capillary forces may not be strong enough to displace much of the oil in the largest pores, but the viscous forces in the forced water imbibition may be able to displace some of this oil. Because different pore sizes may have different fluid distributions, and spontaneous and forced water imbibition may not have the same impact on various pore sizes, the average fluid distribution in a core plug may not correspond for the two displacement processes. In other words, it may be the heterogeneities in the core plug giving the reversal in T_2 shift for the oil phase after forced water imbibition. The fact that the reversed shift is not seen for all of the imbibition cycles may also reflect the heterogeneity of the rock material.

MRI measurements during forced water imbibition may contribute to the understanding of fluid distributions in these samples. The uppermost curve in Figure 5a gives the signal intensity along the core length for the un-aged core plug HR27 at residual water saturation. D_2O is utilized as the water phase, so that the observed signal comes only from the oil in the core plug. The signal intensities are averages calculated based on cross sections of the core plug from 3D images. The intensity profile at residual water saturation is relatively uneven, suggesting that there is an unequal distribution of porosity and/or oil saturation along the core length. As the injection of D_2O starts, a decrease in signal intensity is seen near the inlet end of the core. In Figure 5b, the signal intensity at each core length is normalized to the signal intensity at residual water saturation, giving the relative change in signal intensity between each image. Because some of the irregularities in the signal intensity curves are repeated as the water flooding takes place, the uneven curve at residual water saturation probably reflects heterogeneities in porosity and not in oil saturation. It is seen from Figure 5b that the water front is relatively dispersed, reflecting some of the heterogeneity of the core plug. But there does not seem to be very large irregularities along the core length.

Local variations in the core plug may be further investigated by obtaining T_2 distributions on predefined slices of the core plug. This method has shown to give promising results when applied on Portland chalk, Johannesen *et al.*, (2008). T_2 distributions are obtained for three different slices on 6 cm long core plugs. The thickness of the slices is 2 cm. Two of the slices cover the core volume from the centre of the core length to 1 cm from each of the ends, while the third slice is taken at the centre of the core. This means that the third slice overlaps the two other slices. T_2 values for the oil peak (a), average signal intensity from

the three first data points in the decay curve (SIZE) for each gradient measurement (b), water saturation calculated based on T_2 distributions (c) and all the T_2 distributions obtained by fixed gradient and non-gradient measurements at residual water saturation (d) are shown in Figure 6.

During the first part of the imbibition, the T_2 for the oil phase seems to decrease for the whole core plug (Figure 6a). Since the T_2 for the oil phase at residual water saturation is lower than bulk decane, parts of the oil phase have to be in contact with the pore walls. When the water phase increases in the core plug, the oil droplets decrease, but are still in contact with parts of the pore walls. When the water saturation exceeds 43%, it seems like the T_2 for the oil phase starts increasing. The reason for the increase could be that the contact between the oil and the pore walls decreases more than the oil volume (see Equation (1)). The T_2 for the oil phase approaches the value for bulk decane, and for the two last saturation states, the oil phase has higher T_2 values than bulk decane, as mention earlier during the discussion of the results in Figure 2. Unequal distribution of fluid saturations, pore sizes and density of paramagnetic ions in the pore walls may give different T_2 distributions for the various core slices. Except for the two last saturation states, there does not seem to be large T_2 variations for the oil phase along the core length.

Because the signal intensity is proportional with the number of hydrogen nuclei, a glance at Figure 6b may give impression of lower porosity near the ends of the core plug compared to the cores centre. However, this is not the case. The main reason for the large variations in signal intensity is effects from the measuring technique. When obtaining T_2 distribution on predefined slices of the core plug, the resonance frequency is set to match the magnetic field strength in the centre of the core slice. Some of the hydrogen nuclei outside the desired slice may also respond at the set resonance frequency, but the response decreases as the distance to the slice centre increases. When measuring on the slice near the ends of the core plug, larger fraction of the volume outside the predefined slice responding at the set resonance frequency are from the air outside the core plug, compared to the centre slice of the core plug. Because the air has smaller hydrogen density than the fluids in the core plug, the total signal intensity decreases when moving from the centre of the core length towards the ends. The differences in signal intensity along the core length do therefore not give any valuable information which may be applied in the interpretation of the T_2 distributions.

Studying Figure 6c, there seem to be non-uniform fluid distribution within the core plug at residual water saturation. The flooding of the core plug, with 10 PV decane from both directions (5 PV one direction, 10 PV the opposite direction and then 5 PV the first direction), should ensure uniform saturation distribution. The dome shape of the water saturation curve at residual water saturation may reflect some of the uncertainty in the measurements. The water saturations are obtained by summarizing the signal intensity of the water peaks in the T_2 distributions and divide it by the total intensity of the whole T_2 distribution curve. It is seen from the water saturation plot that the water saturation increases for the whole core plug during the water imbibition, except for the saturation

state equal 46%. The curve may reflect the uncertainty in the measurements. The water saturations obtained from T_2 measurements without any gradient field (curve labels) show small changes in overall saturations at this point in the imbibition. The data points in the last (uppermost) curve in the diagram are obtained after forced water injection. 5 PV of water are injected in both directions (4 PV one direction, 5 PV the opposite direction and then 1 PV the first direction). As for residual water saturation, it does not seem like there is uniform saturation distribution through the core plug, but the differences along the core plug are smaller at residual oil saturation.

The last diagram in Figure 6 shows the T_2 distributions for the three core slices together with that obtained for the whole core plug. Because there are more diffusion effects for the results obtained with an additional gradient field, it may be difficult to compare results obtained with and without this gradient field. Figure 7 shows T_2 distributions obtained for centre slices of various thicknesses for a 100% water saturated core plug, together with the T_2 distribution obtained for the whole core plug (without any gradient field). A trend towards faster relaxation times when the slice thickness decreases is seen for the two largest peaks in the T_2 distributions, because narrower slices require stronger gradient fields (which give larger diffusion effects according to Equation (1)). However, there seems to be very good agreement for the relaxation times for the oil phase at residual water saturation.

CONCLUSIONS

- Both H_2O and D_2O has been utilized as water phase in water imbibition of un-aged Edwards Limestone core plugs in order to distinguish the signal from the oil phase from the water phase in the T_2 distributions at different water saturation states. The results showed that there was no overlapping of signal from the two fluid phases in the core plug, meaning that the T_2 distributions alone may give the fluid saturations.
- Poor reproducibility of imbibition curves and relative shifts in T_2 distributions indicates that Edwards Limestone is a rather heterogeneous rock material.
- The technique of measuring T_2 distributions on predefined slices of the core plug needs to be further investigated in order to give valuable information about a heterogeneous rock material.

NOMENCLATURE

D = self diffusion coefficient of fluid, cm^2/s
G = magnetic field gradient, gauss/cm
PV = pore volume
SIZE = average signal intensity of the three first data points in the NMR decay curve
S_w = water saturation
S_{wi} = residual water saturation
S_{wor} = water saturation at residual oil saturation
S = pore surface area, m^2
T_2 = spin-spin relaxation time, s
T_{2b} = relaxation time for pore bulk, s
T_{2s} = relaxation time for pore surface, s
t_E = time between echoes, s
V = pore volume, m^3
wt% = weight percent
δ = thickness of pore surface area
γ = gyromagnetic ratio, Mhz/T

REFERENCES

1. Amott, E., "Observations Relating to the Wettability of Porous Rock", *Trans., AIME*, (1959), **216**, 156-162.
2. Boneau, D.F. and Clampitt, R.L., "A Surfactant System for the Oil-Wet Sandstone Of the North Burbank Unit", *JPT*, (1977), **29**, 5, 501-506.
3. Carr, H.Y. and Purcell, E.M., "Effects of Diffusion on Free Precession in Nuclear Magnetic Resonance Experiments", *Phys. Rev*., (1954), **94**, 3, 630-638.
4. Chang, D. and Ioannidis, M. A., "Pore Network Simulation of Low-Field NMR Relaxometry under Conditions of Drainage and Imbibition: Effects of Pore Structure and Saturation History", *Petrophysics*, (2002), **43**, 4, 376-382.
5. Ding, M., Kantzas, A. and Lastockin, D., "Evaluation of Gas Saturation During Water Imbibition Experiments", *JCPT*, (2006), **45**, 10, 29-35.
6. Dunn, K.-J., Bergmann, D.J. and Latorraca, G.A., "*Nuclear Magnetic Resonance Petrophysical and Logging Applications",* Elsevier Science Ltd., Oxford, UK (2002), 71-95.
7. Howard, J.J., and Spinler, E.A., "Nuclear Magnetic Resonance Measurements of Wettability and Fluid Saturations in Chalk", *SPE Advanced Technology Series,* (1995), **3**, 1, 60-65.
8. Johannesen, E.B., Steinsbø, M., Howard, J.J. and Graue A., "Wettability Characterization by NMR T_2 Measurements in Chalk", *International Symposium of the Society of Core Analysts, 12-16 September 2006, Trondheim, Norway*, (2006).
9. Johannesen, E.B., Riskedal, H., Tipura, L., Howard, J.J. and Graue, A., "Wettability Characterization by NMR T_2 Measurements in Edwards Limestone Rock", *International Symposium of the Society of Core Analysts, 10-13 September 2007, Calgary, Canada*, (2007).
10. Johannesen, E.B., Howard, J.J. and Graue, A., "Evaluation of Wettability Distributions in Experimentally Aged Core Samples", *International Symposium of the Society of Core Analysts, 29 October-2 November, 2008, Abu Dhabi, UAE,* (2008).
11. Kenyon, W.E., "NMR as a Petrophysical Measurement", *Nucl. Geophys*., (1992), **6**, 2, 153-172.
12. Meiboom, S. and Gill, D., "Modified Spin-Echo Method for Measuring Nuclear Relaxation", *Rev. Sci. Instrum*., (1958), **29**, 8, 668-691.
13. Straley, C., Morriss, C. E., Kenyon, W. E. and Howard, J. J., "NMR in Partially Saturated Rocks: Laboratory Insights on Free Fluid Index and Comparison with Borehole Logs", *The Log Analyst*, (1995), **35**, 1, 40-56.

Table 1. Fluid data.

Fluid	Type/Content	Density at 20°C, [g/cm^3]	Viscosity at 20°C, [cP]
Brine	Distilled water 5 wt% NaCl 5 wt% $CaCl_2$	1.06	1.09
D_2O	D_2O 5 wt% NaCl 5 wt% $CaCl_2$	1.18	1.09
n-Decane ($C_{10}H_{22}$)	Mineral oil	0.73	0.92

Table 2. Core plug data.

Core	Length [cm]	Diameter [cm]	Porosity	Permeability [mD]	Amott-Harvey index
HR27	6.14 ± 0.01	3.83 ± 0.01	0.18 ± 0.03	6.76 ± 0.07	
HR28	5.95 ± 0.01	3.80 ± 0.01	0.17 ± 0.03	6.53 ± 0.05	1.0 ± 0.2
HR29	5.93 ± 0.01	3.80 ± 0.01	0.18 ± 0.03	6.74 ± 0.05	0.9 ± 0.2
HR36	5.91 ± 0.01	3.80 ± 0.01	0.20 ± 0.03	13.7 ± 0.3	

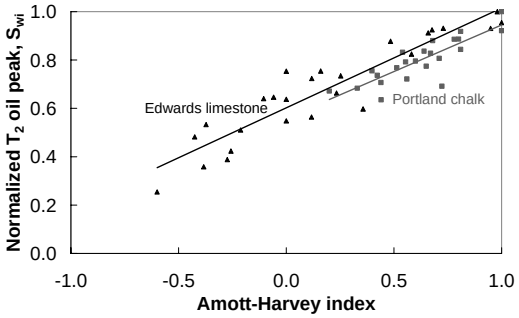

Figure 1. Normalized T_2 for the oil phase at residual water saturation versus Amott-Harvey index for 26 Edwards Limestone core plugs and 23 Portland chalk core plugs.

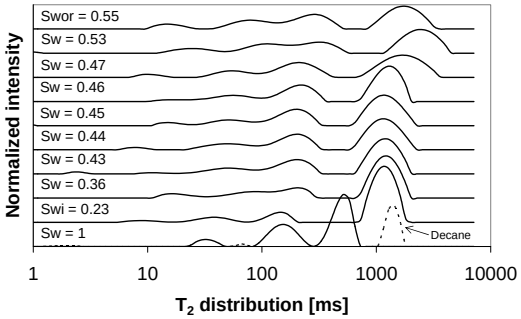

Figure 2. T_2 distributions for an core plug (HR29) at different saturations during spontaneous water imbibition and at end point saturations.

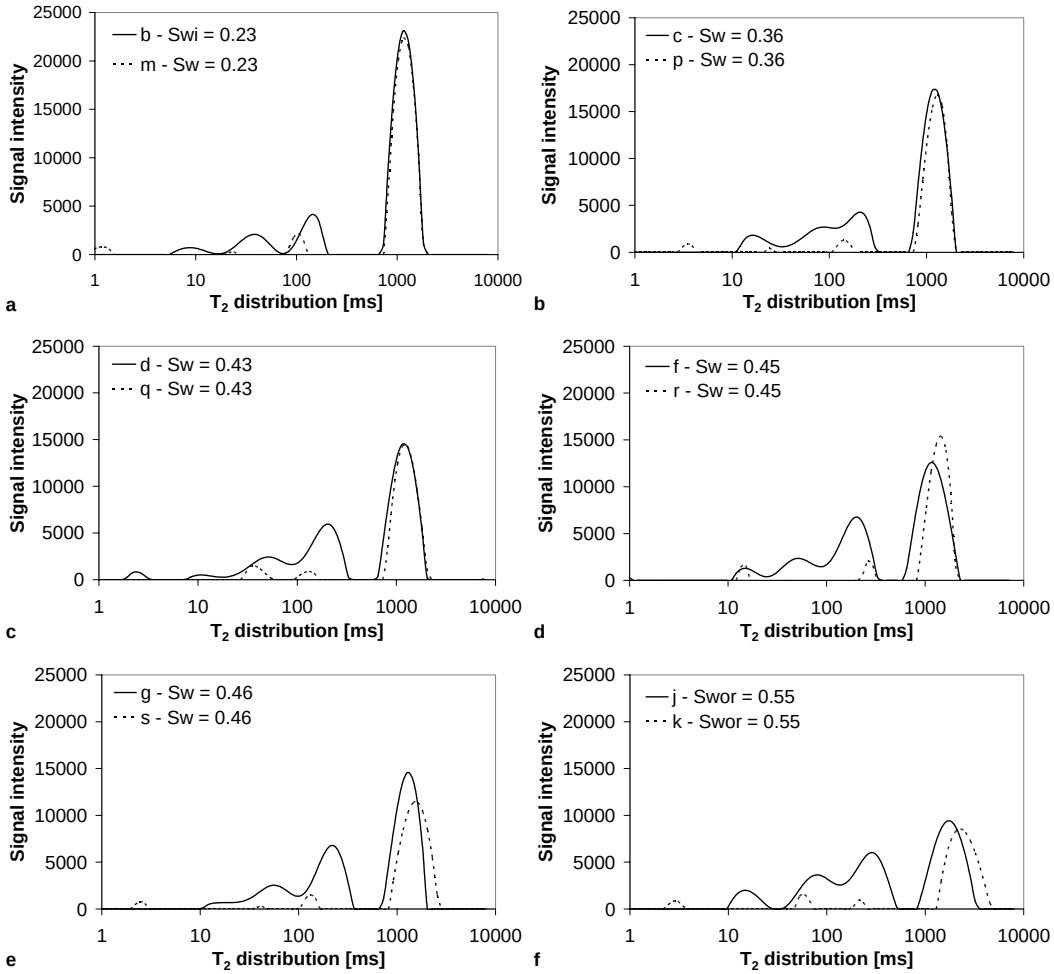

Figure 3. Comparison of T_2 distribution curves for H_2O imbibition (solid lines) and D_2O imbibition (dotted lines) for the core plug HR29, at six different saturation states.

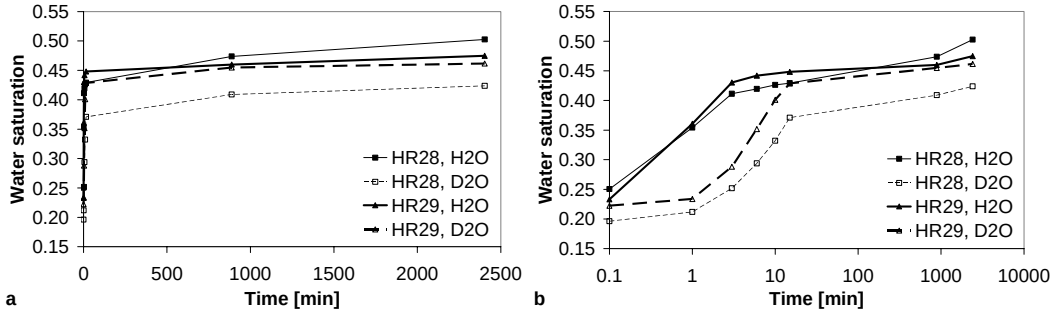

Figure 4. Increase in water saturation during spontaneous water imbibition using H_2O and D_2O respectively as water phase, for the two core plugs HR28 and HR29, with a) linear time axis and b) logarithmical time axis.

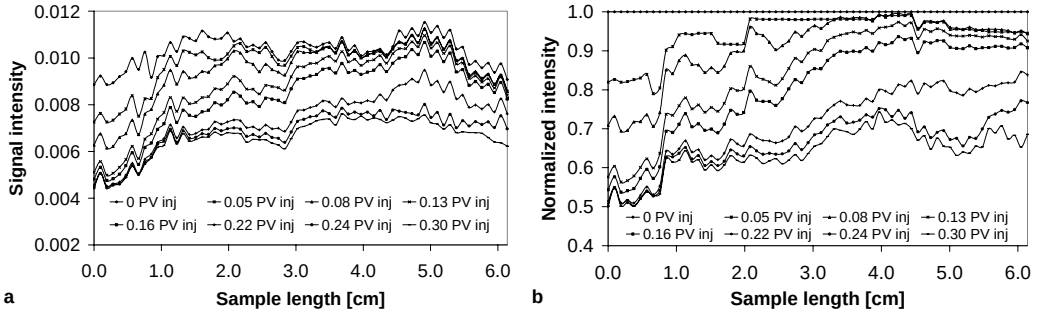

Figure 5. a) Signal intensity and b) normalized signal intensity versus core plug length for the core plug HR27 flooded by D_2O from left.

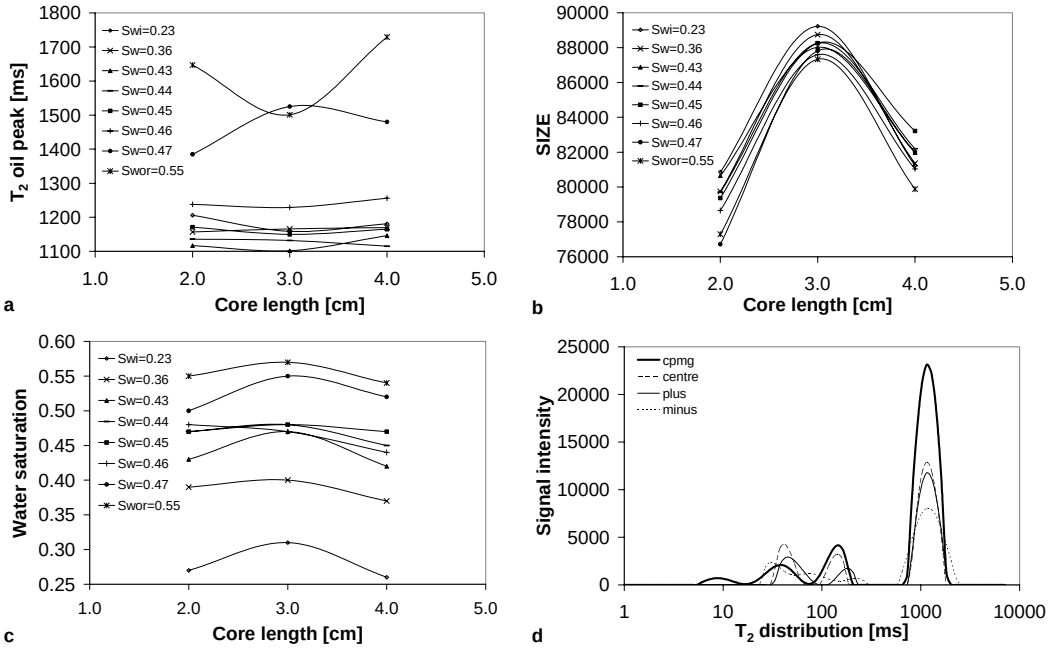

Figure 6. a) T_2 values for the oil phase, b) SIZE values and c) water saturations calculated from T_2 distributions, obtained by gradient measurements during water imbibition in the core plug HR29. d) T_2 distributions with and without gradient field at residual water saturation in HR29.

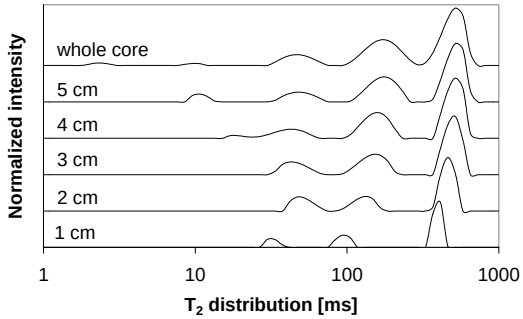

Figure 7. T_2 distributions for centre slices of different thicknesses obtained for the water saturated core plug HR36.